GEOTAIL, POLAR, WIND, CANOPUS, AND ISTP ASSOCIATED GEOSYNCHRONOUS SATELLITE OBSERVATIONS OF PLASMA WAVE EMISSIONS AND RELATED MAGNETOSPHERIC PHENOMENA DURING SUBSTORMS

R. R. Anderson, D. A. Gurnett, L. A. Frank, and J. B. Sigwarth
The University of Iowa, Department of Physics and Astronomy, Iowa City, IA 52242, USA

H. Matsumoto, K. Hashimoto, and H. Kojima
Radio Atmospheric Science Center, Kyoto University, Uji, Kyoto 611, Japan

Y. Kasaba
Department of Electronics and Information, Toyama Prefectural University, Kosugi, Toyama 939-03, Japan

M. L. Kaiser
NASA/Goddard Space Flight Center, Greenbelt, MD 20771, USA

G. Rostoker
Department of Physics, University of Alberta, Edmonton, Alberta, Canada T6G 2JI

J.-L. Bougeret and J.-L. Steinberg
DESPA-URA CNRS 264, Observatoire de Paris-Meudon, F-91295 Meudon Cedex, France

I. Nagano
Department of Electrical and Computer Engineering, Kanazawa University, Kanazawa 920, Japan

T. Murata
Department of Computer Physics, Ehime University, Bunkyocho 3, Matsuyama 790, Japan

H. J. Singer and T. G. Onsager
Space Environment Center, NOAA, Boulder, CO, 80303, USA

M. F. Thomsen
Los Alamos National Laboratory, Los Alamos, New Mexico, 87545, USA

Abstract. Several plasma wave emissions observed by GEOTAIL, POLAR, and WIND are related to substorms. Comparison of the wave characteristics between the three ISTP spacecraft as well as to other space and ground substorm observations allows us to study both the sources of the waves and the plasma dynamics. Auroral kilometric radiation (AKR) has long been known to be related to geomagnetic activity. Observations from multiple spacecraft aid us in separating differences in the AKR spectra due to generation or propagation effects. Low frequency (LF) bursts are a part of AKR observed during strong isolated substorms detected by the CANOPUS and other magnetometer networks. We have found that more high frequency AKR is detected by either GEOTAIL or WIND during LF burst events only if the path from the AKR source is not blocked by the earth or dense plasmasphere. POLAR observations from high over the AKR source region show that the AKR increases in intensity and its lower frequency limits decrease when LF bursts are observed indicating that the AKR source region is expanding to higher altitudes. Frequently the upper frequency limit also increases indicating that the source region is then also expanding to lower altitudes. Images from the POLAR VIS Earth Camera operating in the far-UV range usually feature a strong enhancement in the aurora at the time of the LF bursts. CANOPUS ground magnetometer and meridian scanning photometer data show that during the LF burst events the expansive phase onset starts at unusually low latitudes and moves poleward. The data also show that the LF bursts occur when the expansive phase onset signatures are most intense. Many of the LF bursts occurred related to CME events observed by SOHO which were later identified by the NOAA SEC as being highly geoeffective. Large injections of protons and electrons have also been detected by the GOES and LANL geosynchronous satellites during LF burst events. For one event a sudden injection of energetic

SUBSTORMS-4, Edited by S. Kokubun and Y. Kamide.

electrons was detected by the LANL 1991-080 satellite near dusk simultaneous with POLAR VIS observations of auroral brightening near the magnetic footprint of the LANL satellite. Plasma wave observations from GEOTAIL, POLAR, and WIND of continuum storms and enhanced escaping continuum radiation produced by injected plasma drifting around the magnetosphere and impinging on the plasmasphere also help describe plasma motion during substorms.

Introduction

The Plasma Wave and Radio Science experiments on the ISTP spacecraft GEOTAIL [*Matsumoto et al.*, 1994], WIND [*Bougeret et al.*, 1995], and POLAR [*Gurnett et al.*, 1995] are able to detect in situ and remotely numerous plasma wave phenomena related to geomagnetic storms and substorms. Terrestrial low frequency (LF) bursts are a part of auroral kilometric radiation (AKR) often observed during strong substorms [*Steinberg et al.*, 1988,1990; *Kaiser et al.*, 1996; *Anderson et al.*, 1997,1998]. *Desch et al.* [1996] found using WIND observations that LF bursts were well correlated with high solar wind speeds. GEOTAIL PWI measurements along with those from the WIND/WAVES experiment and the POLAR PWI, POLAR VIS [*Frank et al.*, 1995] imaging data, and CANOPUS [*Rostoker et al.*, 1995] ground observations have provided significant new information on LF bursts and their relation to geomagnetic activity. We have found that LF bursts are intimately related to AKR and many are produced simultaneously with intense isolated substorms as illustrated in the following two cases which independently had been included on a list of highly-geoeffective events compiled by the NOAA SEC and the list of geomagnetic storms caused by coronal mass ejections (CMEs) in *Brueckner et al.* [1998]. We had already begun to study several of the events on these lists because of the distinctive LF bursts they produced.

April 11, 1997, Events

The early part of April 11, 1997, was highly disturbed as a result of ejecta from the April 7 CME passing near Earth [*Berdichevsky et al.*, 1998]. Kp was 7 for the 03-06 UT period [*Brueckner et al.*, 1998]. CANOPUS ground magnetometer data for a six-hour period just prior to the ejecta engulfing Earth are shown in Figure 1. Figure 2 displays the POLAR, GEOTAIL, and WIND plasma wave observations for the same time. POLAR was inbound from apogee to perigee near local midnight. GEOTAIL was at R = 14 R_e in the upstream solar wind just outside the subsolar bow shock. The two lines beginning near 40 kHz and 80 kHz in the GEOTAIL and WIND spectrograms are at F_{pe}, the local electron plasma frequency, and $2F_{pe}$ generated near the Earth's bow shock. WIND was 231 R_e upstream of the Earth (GSM X,Y,Z = 229.7 R_e, 0.5 R_e, 22.9 R_e, R = 230.9 R_e) at 06:00 UT. The F_{pe} line in the WIND data shows that at about 04:32 UT the solar wind

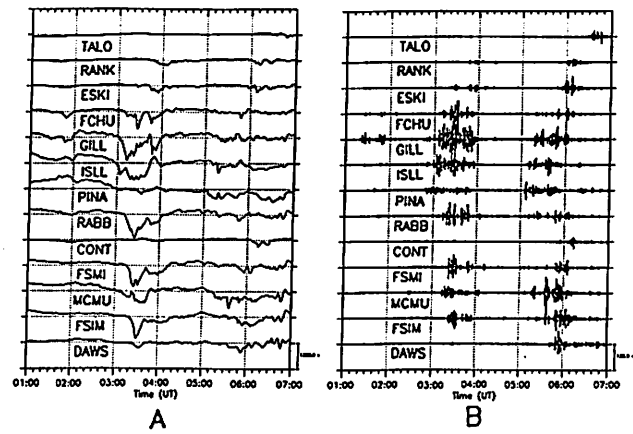

Figure 1. The CANOPUS array magnetometer north-south (X) component data for 0100 UT to 0700 UT on April 11, 1997. Panel A is unfiltered and Panel B is high-pass filtered with f_c = 7 mHz which highlights Pi2 oscillations associated with expansive phase onsets. The locations of the thirteen stations are listed in Table 1.

density abruptly increased from 20 cm^{-3} to about 45 cm^{-3} in a 15-minute period. F_{pe} is equal to 8.98 kHz times the square root of the number density, Ne, in cm^{-3}. This abrupt density enhancement arrived at GEOTAIL near the Earth about 50 minutes later indicating a solar wind speed of 490 km/s. Beginning around 05:50 UT, the density at WIND abruptly dropped to 10 cm^{-3}. *Berdichevsky et al.* [1998] concluded that the CME ejecta embedded in a strong positive Bz interplanetary magnetic field (IMF) swept past WIND from 05:50 UT to ~15:00 UT and was then followed by an interaction region formed ahead of a high-speed stream detected late on April 11. A reverse shock detected at 20:52 UT at WIND was believed to be the trailing edge of this interaction region.

Three periods of heightened geomagnetic activity are evident in the ground magnetograms and in the POLAR electric field spectrogram beginning about 01:15 UT, 02:35 UT, and 04:45 UT, respectively. The second and third produced LF bursts clearly detectable with their diffuse tails in the GEOTAIL and WIND spectrograms beginning

Table 1. CANOPUS Magnetometer Sites

		Geographic		Pace			Inv.
Location	Acronym	Lat.	Long.	Lat.	Long.	L	Lat.
Taloyoak	TALO	69.5	266.4	79.6	-36.4	31.7	79.6
Rankin Inlet	RANK	62.8	267.9	73.7	-29.0	12.4	73.5
Eskimo Point	ESKI	61.1	266.0	71.9	-31.8	10.2	71.7
Fort Churchill	FCHU	58.8	265.9	69.7	-30.8	8.2	69.6
Gillam	GILL	56.4	265.4	67.4	-30.9	6.7	67.3
Island Lake	ISLL	53.9	265.3	64.9	-30.3	5.5	64.8
Pinawa	PINA	50.2	264.0	61.2	-31.6	4.3	61.2
Rabbit Lake	RABB	58.2	256.3	67.8	-45.0	6.9	67.6
Contwoyto Lake	CONT	65.8	248.8	73.4	-61.2	12.4	73.5
Fort Smith	FSMI	60.0	248.1	67.9	-57.3	7.1	68.0
Fort McMurray	MCMU	56.7	248.8	64.8	-54.4	5.5	64.8
Fort Simpson	FSIM	61.7	238.8	67.6	-69.9	6.8	67.4
Dawson	DAWS	64.1	220.9	65.9	-90.1	5.9	65.7

about 02:55 UT, 05:35 UT, and 05:55 UT. The initiation or intensification of AKR observed by an appropriately located satellite high over the night auroral region or in the geomagnetic tail well identifies substorm onset. The horizontal striations from about 100 kHz to 500 kHz, most prominent in the first two hours of the GEOTAIL spectrogram in Figure 2B, are enhanced high frequency escaping continuum radiation. This is a new feature identified associated with geomagnetic disturbances. The second and third periods of enhanced AKR agree well with the expansive phase onsets indicated in the CANOPUS MPA data in Figure 3 and ground magnetometer data shown in Figure 1. From the time the ejecta arrived at the Earth at 0640 UT until 2200 UT only a few very weak bursts of AKR were detected by POLAR. IMF Bz remained positive at Earth until 2000 UT. Strong AKR was observed by POLAR and GEOTAIL beginning at 2200 UT shortly after the reverse shock reached Earth.

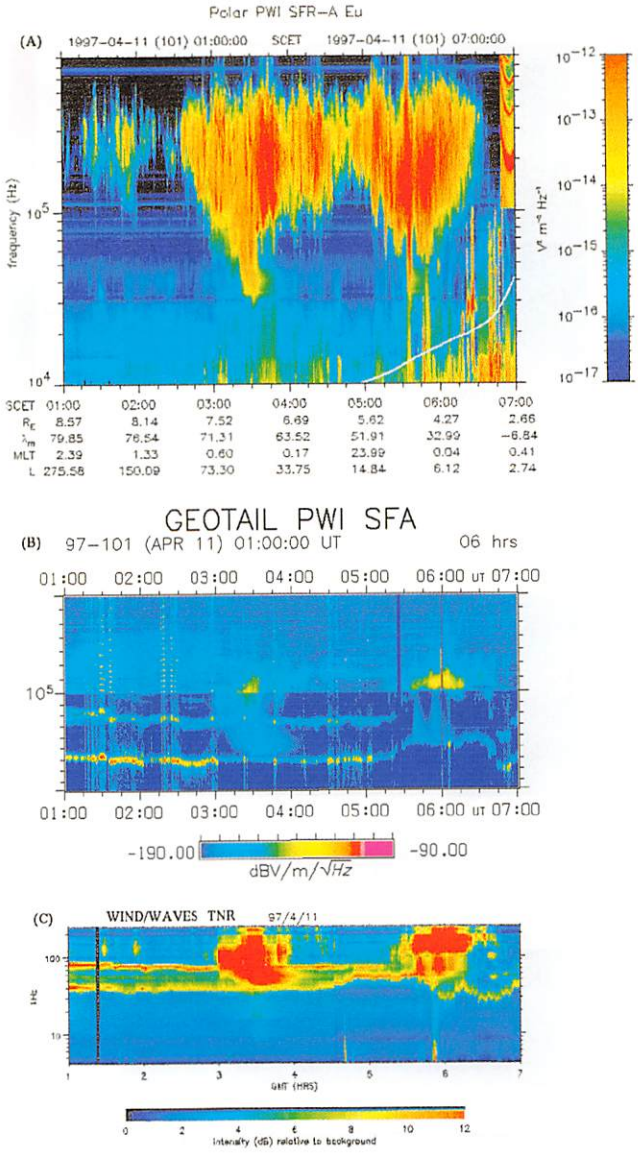

Figure 2. POLAR, GEOTAIL, and WIND color spectrograms of the plasma wave electric field data for 0100 UT to 0700 UT on April 11, 1997. Panel A shows the POLAR Sweep Frequency Receiver (SFR) data plotted logarithmically from 10 kHz to 800 kHz. The plotted dynamic range is 50 dB. The white line identifies the electron cyclotron frequency determined from the POLAR Magnetic Field Investigation (MFI). The strong signals above 100 kHz after 0648 UT near the end of the plot and just before perigee are preamp oscillations that occur in the highest density regions. Panel B shows the GEOTAIL PWI Sweep Frequency Analyzer (SFA) electric field data plotted on linear scales from 12.5 kHz to 100 kHz and from 100 kHz to 800 kHz. The plotted dynamic range is 100 dB. Panel C shows the WIND/WAVES Thermal Noise Receiver (TNR) plotted logarithmically from 4 kHz to 256 kHz. The plotted dynamic range is 12 dB.

May 15, 1997, Event

Much of mid-day on May 15, 1997, was highly disturbed due to a CME observed by SOHO on May 12 [*Brueckner et al.*, 1998]. Kp was 7 for 09-15 UT. The CANOPUS Electrojet indices in Figure 4 show strong geomagnetic activity during much of the middle of the day. Figure 5 displays the POLAR, GEOTAIL, and WIND plasma wave

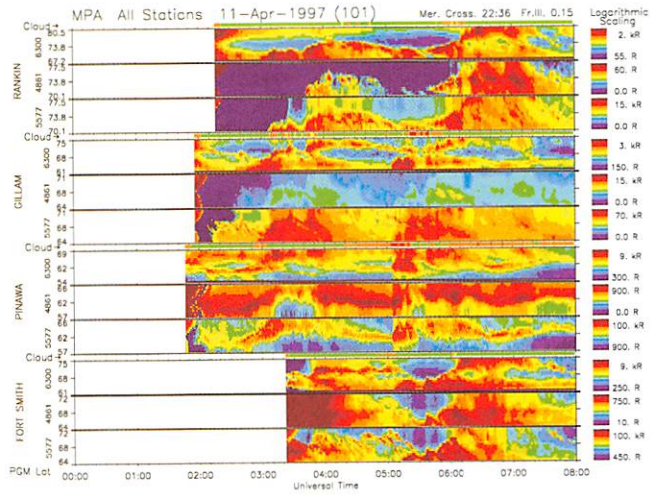

Figure 3. CANOPUS Meridian Scanning Photometer Array (MPA) data for 00:00 UT to 08:00 UT on April 11, 1997. Pinawa, Gillam, and Rankin Inlet are at progressively higher latitudes on the Fort Churchill line. Fort Smith is slightly north of Gillam but 26 degrees in longitude to the west. The enhanced oxygen 5577 emissions begin around 02:35 UT and 05:05 UT in the Pinawa data at about 60 degrees invariant latitude and move to progressively higher latitudes. These enhanced emissions are indicative of expansive phase onsets.

observations for a two-hour period beginning at noon. AKR emissions from 100 kHz to 400 kHz dominate the POLAR spectrogram and reflect the strong geomagnetic activity present. Near 13:00 UT, the AKR detected by all three spacecraft becomes enhanced and quickly and briefly extends down to below 30 kHz. Expanded POLAR and GEOTAIL spectrograms are shown in Figure 6. The diagonal striations in the AKR and in the LF burst down to about 35 kHz indicate spin modulation and a compact source region. A diffuse tail below 35 kHz is evident after 12:57 UT.

Significant differences are observed in Figure 4 for the particle measurements from the various geosynchronous spacecraft as well as magnetic field measurements from GOES 8 and 9 near 13:00 UT when the LF burst was detected. A strong injection of energetic electrons was detected near 17.6 hrs LT just before 13:00 UT as shown in Figure 7 coincident with the LF burst. At the same time, auroral images from the POLAR VIS instrument show a strong auroral enhancement near dusk [Figure 8].

Discussion and Summary

A common feature of our research is that the AKR increases in intensity and its lower frequency limit decreases when LF bursts are observed indicating that the AKR source region is expanding to higher altitudes. Since AKR is generated near the local electron cyclotron frequency, F_{ce}, the frequency of AKR identifies the location along a magnetic field line where it is generated and the lower the frequency, the higher the altitude. On a 71 degree invariant latitude field line typical for an AKR source region, F_{ce} equals 500 kHz at a geocentric radial distance of 1.47 R_e, 400 kHz at 1.58 R_e, 300 kHz at 1.74 R_e, 200 kHz at 1.98 R_e, 100 kHz at 2.47 R_e, 50 kHz at 3.09 R_e, and 30 kHz at 3.60 R_e. Frequently the upper frequency limit increases

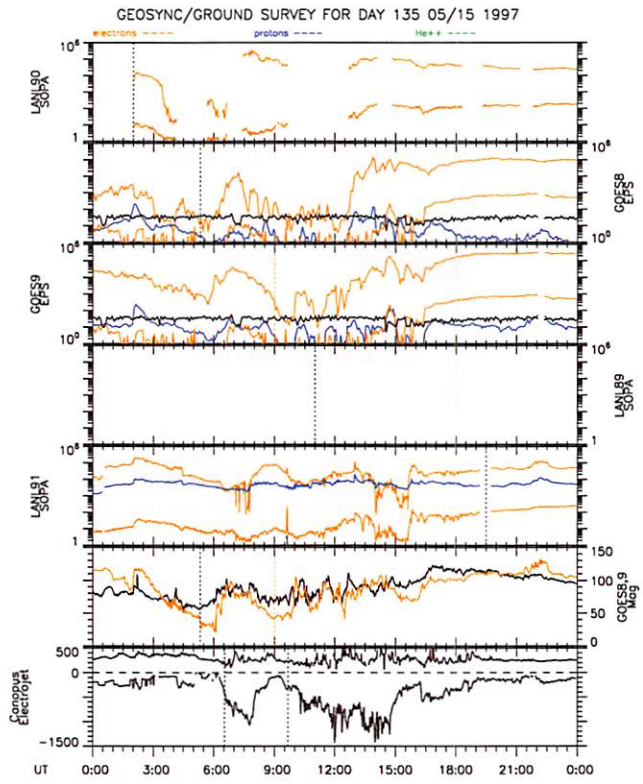

Figure 4. ISTP Geosynchronous and Ground Key Parameter survey plots for May 15, 1997.

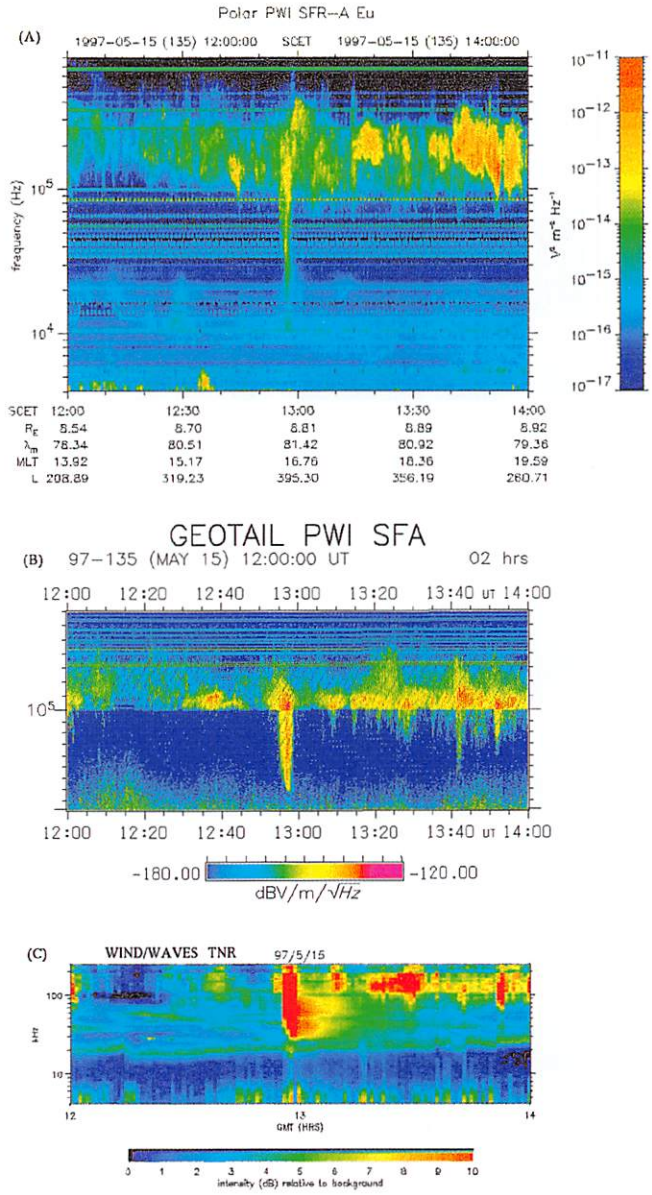

Figure 5. POLAR, GEOTAIL, and WIND spectrograms of the plasma wave electric field data for 1200 UT to 1400 UT on May 15, 1997, 97-135. Panel A shows the POLAR PWI SFR-A Eu spectrogram from 4 kHz to 800 kHz. At 13:00 UT, POLAR was at 8.8 Re, 81 degrees Magnetic Latitude, and 17 hrs MLT. The plotted dynamic range is 60 dB. Panel B shows the GEOTAIL PWI SFA spectrogram from 12.5 kHz to 800 kHz. GEOTAIL was in the magnetosheath near dusk (at 13:00 UT, GSM X,Y,Z = 7.7 Re, 28.7 Re, -0.5 Re, R = 29.7 Re, MLT = 17 hrs, and magnetic latitude = -0.9 degrees). The plotted dynamic range is 60 dB. Panel C shows the WIND/WAVES TNR spectrogram from 4 kHz to 256 kHz. WIND was 190 Re upstream of the Earth (GSM X,Y,Z = 189.6 Re, 2.2 Re, 17.4 Re, R = 190.4 Re) at 13:00 UT. The plotted dynamic range is 10 dB.

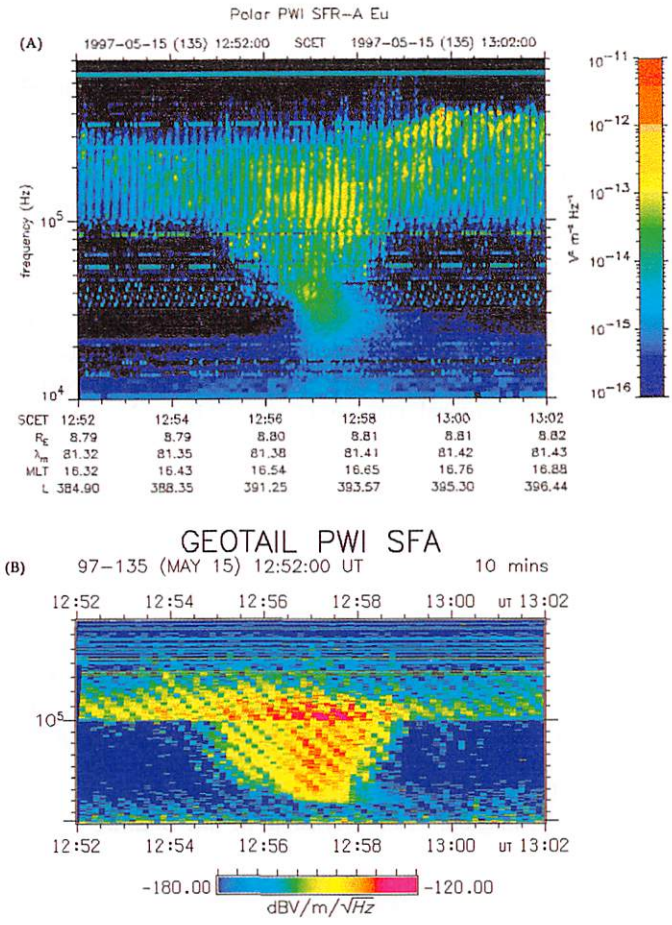

Figure 6. POLAR and GEOTAIL spectrograms for 12:52 UT to 13:02 UT on May 15, 1997, 97-135. Panel A shows the POLAR PWI Electric Field SFR-A Eu spectrogram from 10 kHz to 800 kHz. The plotted dynamic range is 50 dB. Panel B shows the GEOTAIL PWI Electric Field SFA spectrogram from 12.5 kHz to 800 kHz. The plotted dynamic range is 60 dB.

indicating that the source region is then also expanding to lower altitudes. The average speed for the upward movement of the AKR source region for the second event on April 11, 1997, is 3 km/s based on the AKR frequency starting at 300 kHz at 02:34 UT and the lower cutoff falling to 50 kHz by 03:22 UT. The single LF burst observed on May 15, 1997, had an upward AKR source speed of 80 km/s based on the AKR lower cutoff frequency starting at 100 kHz at 12:55 UT and falling to 30 kHz in only 1.5 minutes. A very interesting characteristic of some of the LF bursts we have studied, including those on April 11, 1997, is that they occur as a part of a series of quasi-periodic AKR bursts that progressively extend to lower frequencies. After the LF burst occurs, a series of quasi-periodic AKR bursts that progressively extend to higher frequencies follows.

The absence of the higher frequency AKR in the upstream observations of the LF bursts is due to propagation blockage by the Earth and dense plasmasphere of the portion of the AKR generated at the lowest altitudes on the night side. In Figure 2, the LF burst observed beginning at 05:55 UT on GEOTAIL is not evident on POLAR because the lowest AKR frequencies are refracted away first as POLAR approaches the plasmasphere. These omissions are why we attempt to include observations from as many spacecraft as possible in studying AKR and LF bursts.

Many of the LF bursts we have studied, including the ones in this report, were related to CME events observed by SOHO which were identified by the NOAA SEC as being highly geoeffective. We have found that when LF burst events occurred during night in Canada, the negative bays observed in the CANOPUS magnetometer data were typically around or exceeded -1000 nT. The negative bays around 03:30 UT on April 11, 1997, reached about -1300 nT. In a limited number of cases that we have been able to examine in detail when it was night in Canada, the

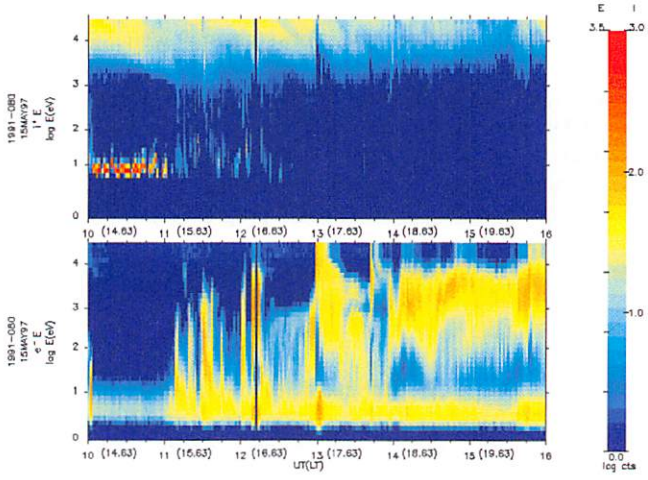

Figure 7. Energy-Time spectrograms of the ion (upper panel) and electrons (lower panel) detected by the LANL Magnetospheric Plasma Analyzer (MPA) experiment on the 1991-080 satellite for 10:00 UT to 16:00 UT on May 15, 1997. The figures in brackets indicate the Local Time position at the hour tic marks.

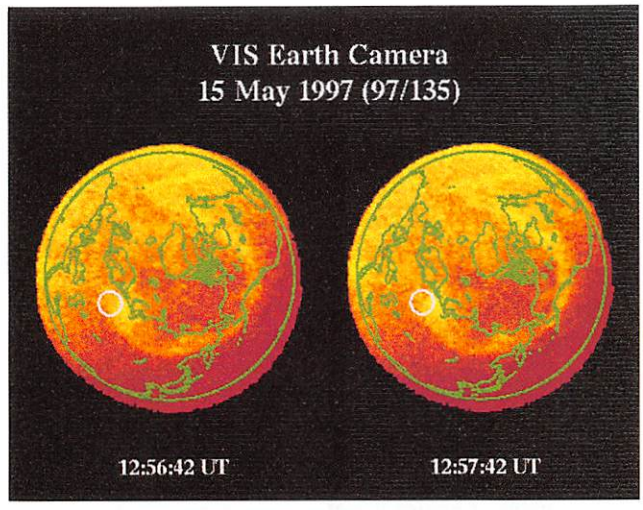

Figure 8. Two POLAR VIS Earth Camera UV images for May 15, 1997. The white circle is the geomagnetic footprint of the LANL 1991-080 satellite.

CANOPUS ground magnetometer and MPA data show that during the LF burst events the expansive phase onsets start at unusually low latitudes and move poleward and westward. The data also show that the LF bursts occur when the expansive phase onset signatures are most intense.

Enhanced continuum radiation typically in the 10 kHz to 100 kHz range is a common feature that follows modest substorm onsets by a few tens of minutes and is due to injected electrons drifting around and encountering the plasmasphere [*Filbert and Kellogg*, 1989; *Kasaba et al.*, 1997]. The current observations in Figure 2B are unusual in that the duration is long, more than two hours, and that the emissions extend to a much higher frequency which indicates that the injected electrons are penetrating much deeper into the plasmasphere. The emissions are generated near odd half harmonics of F_{ce} nearest the local F_{pe}. The higher F_{pe}s are located at smaller geocentric radial distances.

For the April 11, 1997, event, the enhanced plasma wave activity and very disturbed geomagnetic conditions continued until the solar wind density enhancement abruptly declined and the interplanetary magnetic field (IMF) near the Earth turned northward as the ejecta arrived. For the following 13-hour period when the IMF Bz remained positive almost no AKR was detected and no significant geomagnetic activity occurred. Strong AKR was again observed two hours after the IMF turned southward. The May 15, 1997, event occurred during a period of extended geomagnetic activity. As we move towards Solar Maximum, we will have many more opportunities to continue the investigation of the global activity that is associated with and leads to AKR intensification and LF bursts and enhanced escaping continuum radiation. Observations of these phenomena will be used to infer the plasma dynamics associated with substorms.

Acknowledgements. The research at The University of Iowa was supported by NASA Grant NAG5-2346 and NASA Contract NAS5-30371 both with Goddard Space Flight Center.

References

Anderson, R. R., D. A. Gurnett, H. Matsumoto, K. Hashimoto, H. Kojima, Y. Kasaba, M. L. Kaiser, G. Rostoker, J.-L. Bougeret, J.-L, Steinberg, I. Nagano, and H. Singer, Observations of low frequency terrestrial type III bursts by GEOTAIL and WIND and their association with isolated geomagnetic disturbances detected by ground and space-borne instruments, *Planetary Radio Emissions IV*, Proc. Graz Conf., ed. by H. O. Rucker, S. J. Bauer, and A. Lecacheux, Austrian Academy of Sciences Press, Vienna, 241-250, 1997.

Anderson, R. R., D. A. Gurnett, H. Matsumoto, K. Hashimoto, H. Kojima, G. Rostoker, I. Nagano, Y. Kasaba, S. Kokubun, and T. Yamamoto, GEOTAIL, POLAR, and CANOPUS observations of plasma waves and geomagnetic activity related to the April 7, 1997, solar flare and coronal mass ejection, *Geophys. Res. Lett.*, submitted for publication, 1998.

Berdichevsky, D., J.-L. Bougeret, J.-P. Delaboudinie, N. Fox, M. Kaiser, R. Lepping, D. Michels, S. Plunkett, D. Reames, M. Reiner, I. Richardson, G. Rostoker, J. Steinberg, B. Thompson, and T. von Rosenvinge, Evidence for Multiple Ejecta: April 7-11, 1997 ISTP Sun-Earth Connection Event, *Geophys. Res. Lett.*, *25*, 2473-2476, 1998.

Bougeret, J.-L., M. L. Kaiser, P. J. Kellogg, R. Manning, K. Goetz, S. J. Monson, N. Monge, L. Friel, C. A. Meetre, C. Perche, L. Sitruk, and S. Hoang, WAVES: The radio and plasma wave investigation on the WIND spacecraft, *Space Sci. Rev.*, *71*, 231-263, 1995.

Brueckner, G. E. , J.-P. Delaboudiniere, R. A. Howard, S. E. Paswaters, O. C. St. Cyr, R. Schwenn, P. Lamy, G. M. Simnett, B. Thompson, and D. Wang, Geomagnetic storms caused by coronal mass ejections (CMEs): March 1996 through June 1997, *Geophys. Res. Lett.*, *25*, 3019-3022, 1998.

Desch, M. D., M. L. Kaiser, and W. M. Farrell, Control of terrestrial low frequency bursts by solar wind speed, *Geophys. Res. Lett.*, *23*, 1251-1254, 1996.

Filbert, P. C., and P. J. Kellogg, Observations of low-frequency radio emissions in the earth's magnetosphere, *J. Geophys. Res.*, *94*, 8867, 1989.

Frank, L. A., J. B. Sigwarth, J. D. Craven, J. P. Cravens, J. S. Dolan, M. R. Dvorsky, P. K. Hardebeck, J. D. Harvey, and D. W. Muller, The visible imaging system (VIS) for the Polar spacecraft, *Space Sci. Rev.*, *71*, 297-328, 1995.

Gurnett, D. A., A. M. Persoon, R. F. Randall, D. L. Odem, S. L. Remington, T. F. Averkamp, M. M. DeBower, G. B. Hospodarsky, R. L. Huff, D. L. Kirchner, M. A. Mitchell, B. T. Pham, J. R. Phillips, W. J. Schintler, P. Sheyko, and D. R. Tomash, The POLAR plasma wave instrument, *Space Sci. Rev.*, *71*, 597-622, 1995.

Kaiser, M. L., M. D. Desch, W. M. Farrell, J.-L. Steinberg, and M. J. Reiner, LF band terrestrial radio bursts observed by Wind/WAVES, *Geophys. Res. Lett.*, *23*, 1283-1286, 1996.

Kasaba, Y., H. Matsumoto, K. Hashimoto, R. R. Anderson, J.-L. Bougeret, M. L. Kaiser, X. Y. Wu, and I. Nagano, Remote sensing of the plasmapause during substorms: GEOTAIL observation of nonthermal continuum enhancement, *J. Geophys. Res.*, in press, 1997.

Matsumoto, H., I. Nagano, R. R. Anderson, H. Kojima, K. Hashimoto, M. Tsutsui, T. Okada, I. Kimura, Y. Omura, and M. Okada, Plasma wave observations with GEOTAIL spacecraft, *J. Geomag. Geoelectr.*, *46*, 59-95, 1994.

Rostoker, G., J. C. Samson, F. Creutzberg, T. J. Hughes, D. R. McDiarmid, A. G. McNamara, A. Vallance Jones, D. D. Wallis, and L. L. Cogger, CANOPUS - A ground-based instrument array for remote sensing the high latitude ionosphere during the ISTP/GGS program, *Space Sci. Rev.*, *71*, 743-760, 1995.

Steinberg, J.-L., C. Lacombe, and S. Hoang, A new component of terrestrial radio emission observed from ISEE-3 and ISEE-1 in the solar wind, *Geophys. Res. Lett.*, *15*, 176-179, 1988.

Steinberg, J.-L., S. Hoang, and J. M. Bosqued, Isotropic kilometric radiation: A new component of the Earth's radio emission, *Ann. Geophysicae*, *8*, pp 671-686, 1990.

Correspondence to: R. R. Anderson (Fax: +1 319 335 1753, E mail: roger-randerson@uiowa.edu)